Equilibrium Swelling Measurements of Network and Semicrystalline Polymers in Supercritical Carbon Dioxide Using High-Pressure NMR

Kristofer J. Thurecht,[†,‡] David J. T. Hill,[‡] and Andrew K. Whittaker*[,†]

Centre for Magnetic Resonance and Department of Chemistry, University of Queensland, Queensland 4072, Australia

Received February 13, 2005; Revised Manuscript Received February 21, 2005

ABSTRACT: The extent of swelling of cross-linked poly(dimethylsiloxane) and linear low-density poly(ethylene) in supercritical CO_2 has been investigated using high-pressure NMR spectroscopy and microscopy. Poly(dimethylsiloxane) was cross-linked to four different cross-link densities and swollen in supercritical CO_2. The Flory−Huggins interaction parameter, χ, was found to be 0.62 at 300 bar and 45 °C, indicating that supercritical CO_2 is a relatively poor solvent compared to toluene or benzene. Linear low-density poly(ethylene) was shown to exhibit negligible swelling upon exposure to supercritical CO_2 up to 300 bar. The effect of CO_2 pressure on the amorphous region of the poly(ethylene) was investigated by observing changes in the ^1H T_2 relaxation times of the polymer. These relaxation times decreased with increasing pressure, which was attributed to a decrease in mobility of the polymer chains as a result of compressive pressure.

Introduction

Supercritical fluids have become an important medium for polymer synthesis, processing, and characterization. In the past decade, supercritical CO_2 has emerged as the most important fluid in this class due to its chemical inertness, easily accessible critical points, noninflammability, low cost, and its classification as a "green" solvent. Indeed, numerous industrial processes now utilize the characteristics of supercritical CO_2 to achieve higher purity and a greater yield in the final product.[1]

One particular area that has prompted considerable interest is the modification of polymer substrates by the incorporation of a secondary polymer or particles. This includes the formation of polymer blends[2−6] and polymer nanocomposites in which the nanoparticles are metals[7,8] or clay.[9] To understand the processes occurring upon inclusion of a secondary species in a polymer substrate, it is important to have an insight into the effects of exposure of the matrix material to supercritical solvents.

It is well-known that supercritical CO_2 is a poor solvent for most polymers. However, despite the low solubility of polymers in the solvent, it has been extensively shown that most polymers will swell in supercritical CO_2.[10−12] In a separate communication we have shown that PDMS fluids swell considerably when exposed to supercritical CO_2.[13] Similarly, blending experiments have shown that semicrystalline polymers show some degree of swelling in this high-pressure solvent.[3]

The solubility of supercritical CO_2 in high-molecular-weight polymers has been investigated in some detail. Indeed, a wide class of semicrystalline polymers including poly(ethylene),[3] poly(propylene),[14] poly(vinyl chloride),[15] and poly(tetrafluoroethylene)[16] have been examined. The intense interest in this class of polymers is due to their suitability and appeal as substrates for the formation of blends. In addition to semicrystalline polymers, recent interest has focused on the swelling of polymer melts upon exposure to supercritical CO_2.[10,17] Poly(dimethylsiloxane) has been well studied due to its intrinsic solubility. Despite considerable investigation of semicrystalline and polymer melts, little research has been focused toward the swelling of elastomeric polymer networks in supercritical CO_2. This class of polymer is of huge importance commercially, and they typically exhibit a high degree of swelling in many solvents.

A number of methods have been proposed to measure polymer swelling at high pressures. Perhaps the most common, and simple, is real-time optical observation of the swelling polymer.[17] This method has been used to observe the swelling behavior of melt-phase polymers upon exposure to supercritical CO_2. However, application of this method to the swelling of solid polymers is difficult due to the inability to accurately measure the small increases in polymer dimensions under pressure. Wynne et al.[18] have used a linear variable differential transformer to measure the swelling of poly(vinylidene fluoride) upon exposure to supercritical CO_2. Neutron reflectivity has also been used to probe the extent of swelling of thin polymer films under high pressure.[19] Recently, Kazarian et al.[20] developed a method of monitoring the swelling of polymers in supercritical CO_2 using high-pressure FTIR imaging. In addition to monitoring the swelling polymer at a resolution of around 15 μm, observation of CO absorption stretches afforded in-situ observation of CO_2 gas sorption. These methods all produce macroscopic data such as swelling isotherms for a particular polymer and solvent system, but secondary information, such as polymer chain dynamics, may not be readily available.

Recently, high-pressure nuclear magnetic resonance has been used to investigate reactions and processes occurring within supercritical solvents.[21−24] In particular, organic reactions involving CO_2 as the reaction medium have been monitored using high-pressure NMR.[25] On the other hand, NMR microimaging at ambient pressure has been shown to be effective in observing the swelling of polymer matrices in conven-

[†] Centre for Magnetic Resonance.
[‡] Department of Chemistry.
* Corresponding author: e-mail A.Whittaker@cmr.uq.edu.au; Fax + 61 7 3365 3833.

10.1021/ma0503108 CCC: $30.25
Published on Web 03/30/2005

Table 1. Density of PDMS Irradiated to Four Different Doses Using γ-rays and a Comparison of the Cross-Link Density Calculated by Swelling Measurements and from the G value

sample	density/ g cm^{-1}	dose/kGy	γ_e/mol g^{-1} (swelling)	γ_e/mol g^{-1} (G(value))
PDMS-250	0.9782	250	6.04×10^{-5}	6.00×10^{-5}
PDMS-550	0.9799	550	1.60×10^{-4}	1.32×10^{-4}
PDMS-750	0.9809	750	2.40×10^{-4}	1.80×10^{-4}
PDMS-1050	0.9819	1050	2.82×10^{-4}	2.52×10^{-4}

tional solvents.[26−28] This method yields very accurate, real-time measurement of the polymer dimensions upon swelling. NMR microimaging can be utilized for obtaining swelling data, and simultaneous measurements can be made to probe the polymer chain dynamics using other NMR pulse sequences. For example, NMR relaxation times can give an insight into polymer chain mobility. Thus, NMR is one of the most versatile methods for investigating the properties of polymers during swelling under high pressure.

In this paper we report the swelling of cross-linked poly(dimethylsiloxane) (PDMS) in supercritical CO_2 and compare it to the effects of this solvent on semicrystalline linear low-density poly(ethylene) (LLDPE). The swelling of cross-linked PDMS upon exposure to supercritical CO_2 was monitored using high-pressure NMR microimaging. In a parallel experiment, the mobility of LLDPE was investigated following exposure to supercritical CO_2 by measurement of NMR relaxation times of the polymer protons as a function of increasing CO_2 pressure.

Experimental Section

Materials. Poly(dimethylsiloxane) (PDMS 200 fluid) was obtained from Dow Corning. The PDMS had a number-average molecular weight of 35 000 Da and a viscosity of 12 500 cSt.[29] Linear low-density poly(ethylene) (LLDPE Dow 2056) was obtained from Dow Chemicals and processed as received. The LLDPE 2056 had average values of M_w and M_n of 110 000 and 26 000, respectively, and contained 15.6 C6 branches per 1000 main-chain carbon atoms, as determined by ^{13}C solution-state NMR.[30] The degree of crystallinity was initially 33% as determined by DSC. This was ascertained by comparison of the enthalpy of melting for the sample to that of a 100% crystalline material (292.65 J g^{-1}).[31]

Preparation of Cross-Linked PDMS. The PDMS 200 sample was irradiated with high-energy radiation to different doses in order to obtain various cross-link densities. γ-Irradiations were carried out in a 220 AECL ^{60}Co facility at room temperature (303 K) in air. The dose rate was 3.47 kGy h^{-1} as measured by Fricke dosimetry. The subsequent PDMS gels were then cut into strips $\sim 1 \times 1 \times 10$ mm^3 to fit inside the high-pressure NMR cell. The densities of the four cross-linked PDMS samples were measured by a helium pycnometer. These are given in Table 1 along with the absolute doses received by each sample.

Analysis. All high-pressure NMR experiments were undertaken in a custom-made NMR cell manufactured from poly(ether ether ketone). The cell was based on the design of Wallen et al.,[32] and details of the cell design will be published elsewhere.[13] The cell is able to fit closely into a 10 mm Bruker birdcage resonator.

High-pressure NMR imaging measurements were carried out on an AMX 300 spectrometer operating at 300.13 MHz for proton nuclei. The swelling of the polymer networks was monitored using a standard Bruker three-dimensional spin echo pulse sequence. The images were acquired using a 90° pulse with duration of 14 μs, an echo time of 7.38 ms, and a repetition time of 2.0 s. The read gradient was 1.5 T m^{-1}, and the images consisted of $128 \times 128 \times 8$ voxels with a slice thickness of 5 mm in a field of view of $1.5 \times 1.5 \times 4$ cm^3. The acquisition time for a single image was 17 min. Typically, the swelling equilibrium was reached in less than an hour after pressurization.

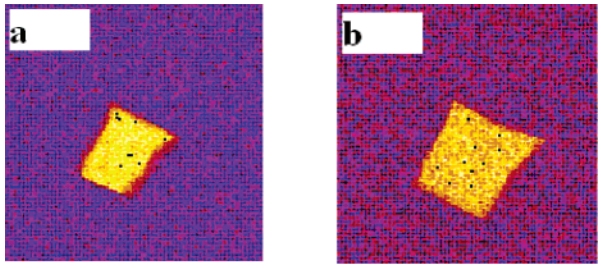

Figure 1. NMR images of a cross section of cross-linked PDMS-250 at equilibrium swelling: 1 bar (a) and 250 bar (b) at 45 °C. The image dimensions are 1×1 cm^2.

High-pressure ^{1}H T_2 relaxation times were performed on an MSL 300 spectrometer operating at 300.13 MHz for proton nuclei. ^{1}H T_2 decays were acquired using the Carr−Purcell−Meiboom−Gill[33,34] pulse sequence with a $\pi/2$ pulse time of 11.5 μs and a τ value ranging from 300 to 1600 μs for PDMS, depending on the extent of swelling and 100 μs for LLDPE. 512 data points were collected, and the signal-to-noise ratio was enhanced by coadding 64 scans with a repetition time of 6 s.

Results and Discussion

Swelling of Radiation-Cross-Linked PDMS. PDMS is distinct among high-molecular-weight polymers, in that it is one of the only known to be readily soluble in supercritical CO_2 at relatively low temperatures and pressures. This inherent solubility of PDMS in supercritical CO_2 advocates PDMS as an interesting polymer for study in this important solvent.

PDMS 200 fluid was irradiated to various doses in order to achieve different cross-link densities. The radiation chemistry of PDMS has been intensely studied by numerous authors over the past half a century.[29,35−37] As a result, the G(value) for cross-linking as well as the mechanism of cross-linking is well-known.[29] The G(value) is a measure of the number of cross-links formed for every 16 aJ of energy absorbed by the sample.[36] When PDMS is exposed to high-energy radiation, it undergoes both scission and cross-linking, with cross-linking processes exceeding the scission. Hill et al.[29,38] showed that both H-linking and Y-linking occurred but that Y-linking predominated. The cross-link density of PDMS increases with received dose; hence, four samples were irradiated to give increasing cross-link densities. The method for calculating the cross-link density is described later in this report. The first sample was irradiated to 250 kGy, just above the gel point (150 kGy)[29] of the fluid (PDMS-250 in Table 1). The largest dose received by the sample was 1050 kGy and represented PDMS in a matrix which has become highly cross-linked and elastomeric (PDMS-1050 in Table 1).

NMR images were acquired of the PDMS samples during exposure to supercritical CO_2. These images show the proton density through a cross section of the polymer. Examples of these images are shown in Figure 1. The degree of swelling for each network as a function of CO_2 pressure is shown in Figure 2. This was calculated from the NMR images by measuring the increase in dimensions of the polymer upon swelling. The sample with the lowest cross-link density has the highest equilibrium swelling at all pressures. Un-cross-linked PDMS would be expected to exhibit an even greater degree of swelling. As the cross-link density increases,

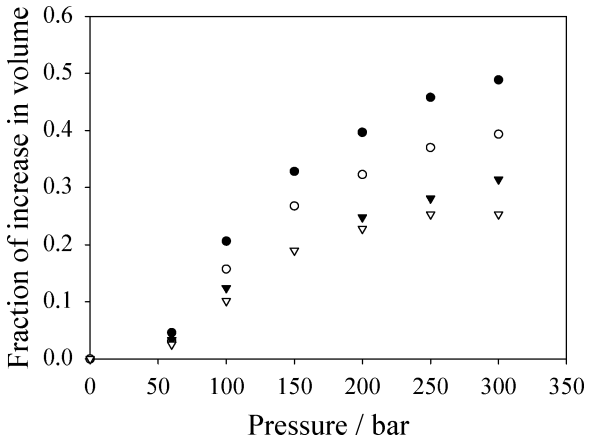

Figure 2. Volume fraction increase of cross-linked PDMS at equilibrium swelling as a function of pressure: PDMS-250 (filled circle), PDMS-550 (open circle), PDMS-750 (filled triangle), and PDMS-1050 (open triangle) at 45 °C.

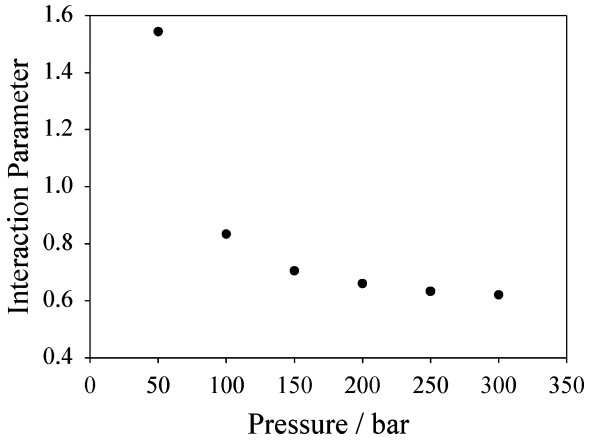

Figure 3. Polymer−solvent interaction parameter, χ, as a function of CO_2 pressure at 45 °C, calculated using the Flory−Rheiner equation for PDMS-250.

a decrease in the degree of swelling is observed. Equilibrium swelling is achieved when the osmotic swelling stresses and the elastic forces due to cross-linking are balanced. This is described quantitatively by the Flory−Rheiner equation (eq 1).[39,40]

The solvent quality of supercritical CO_2 for PDMS was investigated by calculating the Flory−Huggins interaction parameter from the Flory−Rheiner equation.[39,40]

$$\chi = -\frac{\left(\frac{G_e}{RT}\right)v_1 v_2^{1/3} + \ln(1 - v_2) + v_2}{v_2^2} \qquad (1)$$

In eq 1, χ is the Flory−Huggins interaction parameter which is a measure of the quality of a solvent for a particular polymer. G_e is the equilibrium modulus of the unswollen network, v_1 is the molar volume of solvent, and v_2 is the polymer volume fraction at equilibrium swelling. G_e was calculated from the equilibrium swelling ratio of the PDMS networks in toluene, using published values of the interaction parameter.[40,41] The polymer volume fraction (v_2) was determined at each pressure from the NMR images, examples of which are shown in Figure 1. The calculated values of χ are presented for PDMS-250 at various pressures and 45 °C in Figure 3. As the pressure, and hence density, of the solvent increases, the interaction parameter is

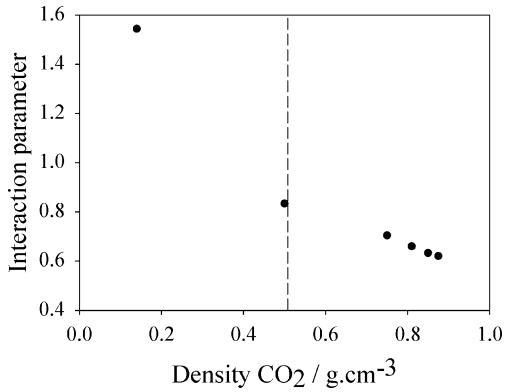

Figure 4. Flory−Huggins interaction parameter, χ, for PDMS-250 as a function of the density of supercritical CO_2 solvent at 45 °C. The vertical dashed line lies at the density of CO_2 at the critical point.

seen to decrease. This is indicative of an increase in solvent power at elevated pressures.

The interaction parameter for PDMS in supercritical CO_2 has a minimum value of 0.62 at 45 °C over the pressure range investigated in this study. This value is significantly higher than that for PDMS in toluene, 0.52, or benzene, 0.55, at the same temperature.[41] This suggests that while the solvent power of supercritical CO_2 significantly increases with pressure, even at the highest density of the fluid used in our investigation, it is still a relatively poor solvent for PDMS. Fleming and Koros[42] measured the sorption of CO_2 into silicone rubber at 35 °C. They showed that at pressures greater than 30 bar the sorption of CO_2 deviated from Henry's law. At higher pressures, the observed nonlinear sorption isotherm was typical of a swelling rubbery polymer, and the behavior was explained using the Flory−Huggins equation. Fleming and Koros[42] calculated a Flory−Huggins interaction parameter of 0.75 for this system at 35 °C; however, the maximum pressure that they could attain using their apparatus was 62 bar, well below the critical pressure of CO_2 (73.8 bar). However, this value is considerably lower than the predicted value of 1 by interpolation of the values plotted in Figure 1. In addition, the interaction parameter measured by Fleming and Koros at 35 °C should be higher than that measured at 45 °C due to temperature effects. This effect is not observed and may be due to differences in the cross-link density of the samples, the effects of which are described later in this report.

The calculated interaction parameters for PDMS-250 at 45 °C have been plotted against the density of supercritical CO_2 in Figure 4. For the region where the CO_2 is a liquid, the density is very low and the solvent is poor. This is denoted by a large interaction parameter for pressures below the critical density for CO_2, 0.468 g cm^{-3}. When the density of the fluid is increased by elevating the pressure, the interaction parameter drastically decreases. This implies that a large increase in the solvent quality of the fluid is attained with an increase in the pressure. Indeed, for densities above the critical density, the interaction parameter decreases approximately linearly with CO_2 density. This is predicted by the Flory−Rheiner equation, eq 1, in which the interaction parameter is directly proportional to the solvent molar volume. Such a dependence highlights the interesting properties of supercritical fluids and the advantages of a highly "density variable" solvent over conventional solvents.

Under the conditions used in this experiment, supercritical CO_2 exists entirely within the so-called "poor" solvent regime. Andre et al.[43] and Melnichenko et al.[44] have shown that for PDMS in supercritical CO_2 a theta temperature ($T_\Theta \sim 60$ °C) and theta pressure ($P_\Theta \sim 520$ bar) exist, beyond which the fluid passes into the so-called "good" solvent regime. Melnichenko et al. used neutron scattering to show that below the theta conditions the radius of gyration (R_g) of the polymer chains was in an unperturbed state; however, above the theta temperature and pressure, the chains expanded and R_g became much larger than the unperturbed dimensions. Indeed, Andre et al. used light scattering to measure the second virial coefficient and showed that the theta temperature decreased with increasing CO_2 density. Unfortunately, the NMR cell used in this current research could not withstand the high temperature and pressure required to reach the theta conditions. Consequently, all of the results presented in this report are for PDMS in supercritical CO_2 in the "poor" solvent regime.

Koga et al.[45] have used neutron reflectivity to investigate the solubility of sc-CO_2 in polymer thin films. Deuterated polymers such as poly(methyl methacrylate), poly(styrene), styrene−butadiene random copolymer, and poly(butadiene) were all investigated. The pressure dependence of the Flory−Huggins interaction parameter was presented and found to be important for these polymers. In all cases, the interaction parameter significantly decreased with increasing pressure. Koga et al. also showed that the solubility of supercritical CO_2 in these polymers increases with increasing CO_2 density.

Numerous methods have been used to determine the cross-link density of polymer networks. Inverse gas chromatography (IGC),[46] dynamical mechanical analysis (DMA),[41] and differential scanning calorimetry (DSC)[47] have all been used to estimate cross-link density. However, special sample preparation, in the case of DMA, and the use of specialized equipment, in the case of IGC and DSC, place limitations on these methods. Estimation of the cross-link density of a polymer network through swelling is perhaps the most commonly used method. The cross-link density (γ_e) is related to the swollen polymer network through the Flory−Huggins interaction parameter as follows:

$$\gamma_e = -2\,\frac{\ln(1-v_2) + \left(1-\frac{1}{r}\right)v_2 + \chi {v_2}^2}{\rho_p v_1 {v_2}^{1/3}} \qquad (2)$$

where ρ_p is the density of the polymer. The cross-link density was calculated using swelling ratios at 300 bar and 45 °C for each of the four irradiated samples. The values are given in Table 1. The molar volume of the solvent under these conditions was calculated to be 50 mL mol^{-1}. These values are compared to the cross-link density calculated using the published G(value) for cross-linking when irradiated in air[37] (Table 1). In all cases, a larger cross-link density is determined from the swelling method. The uncertainty involved in the calculation of the G(value) for PDMS irradiated with high-energy radiation would significantly alter the calculated cross-link density estimated from the G(value) for cross-linking. Hill et al.[37,38] estimated that the minimum overall G(value) for cross-linking would lie between 1.9 and 2.3 under vacuum at 303 K, but it has been estimated to be as high as 3.4.[36] This uncertainty might explain the slightly different results obtained from the swelling measurements.

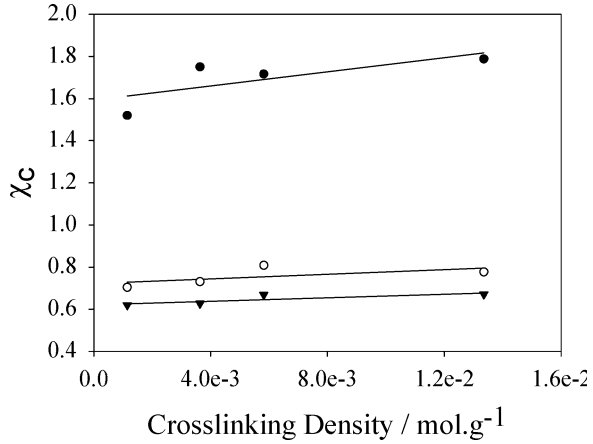

Figure 5. Flory−Huggins interaction parameter, χ, of PDMS in supercritical CO_2 as a function of the cross-link density γ_e at 50 (filled circle), 150 (open circle), and 300 bar (triangle) and 45 °C.

In recent years, numerous reports have provided evidence that the interaction parameter in some systems is not independent of cross-link density.[48−50] McKenna et al.[48,50] and Hrnjak-Murgic et al.[49] showed that significant dependence of the interaction parameter on cross-link density existed for cross-linked natural rubber and ethylene−propylene−diene rubber (EPDM). By utilizing various solvents, McKenna and co-workers showed that the relationship $\chi_c = \chi_o + \alpha\gamma_e$ held for all solvents studied, where c and o denote cross-linked and un-cross-linked polymer, respectively. Indeed, the proportionality constant α was generally found to increase for poorer solvents. For the EPDM system, Hrnjak-Murgic and co-workers found a similar linear relationship between cross-link density and interaction parameter. On the other hand, Malone et al.[40] used measurements of the shear modulus to show that there was no cross-link dependence on the interaction parameter for PDMS when swollen in the good solvents, di- and trimethylpentane.

The effect of cross-link density on the measured interaction parameter for CO_2 and PDMS is shown in Figure 5. Three different densities of supercritical CO_2 are shown, and the data have been fitted to the relationship described by McKenna et al.[48] The intercept of each graph is the extrapolated value for the interaction parameter of virgin PDMS fluid, and the slope is a proportionality constant. For the three experiments shown, both χ_0 and α decrease with increasing solvent density. This is indicative of an improvement in the solvent quality as the density is increased. Indeed, as supercritical CO_2 approaches the "good" solvent regime for PDMS, the proportionality constant approaches unity. This indicates that the cross-link dependence of χ may be zero or negligible for good solvents and concurs with the results of Malone et al.[40]

Polymer Chain Mobility by Measurement of ^{1}H NMR T_2 Relaxation Times. The transverse relaxation time (T_2) of a polymer gives information on the molecular motion of polymer chain segments.[51] Traditionally, spin−spin relaxation times have been used to investigate the relatively slow, large chain-segment motion in polymers.[51,52] ^{1}H T_2 relaxation times were measured for a number of polymers in sc-CO_2 to determine the effect

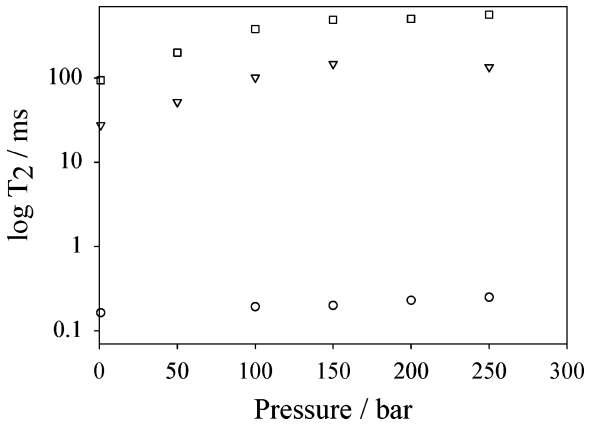

Figure 6. ^{1}H T_2 relaxation times (log scale) measured for cross-linked PDMS-250 as a function of pressure at 45 °C: T_{2s} (circles), T_{2i} (triangles), and T_{2l} (squares).

of pressure on the molecular dynamics of the polymer chains. Initially, the ^{1}H T_2 relaxation times of cross-linked PDMS were investigated as a function of pressure, and the results are shown in Figure 6. The relaxation decay for all four PDMS networks could be resolved into three different relaxation times. The shortest relaxation time (T_{2s}), well below 1 ms, is due to polymer chains that have significantly restricted mobility. This represents those chains physically joined via a cross-linking covalent bond or chain segments adjacent to cross-links. This short relaxation time has also been attributed to chains which are highly entangled and whose motion is subsequently restricted. Indeed, Shim et al.[53] suggested that there is very little difference in transverse relaxation times for those protons in a rigid environment as a result of either cross-linking or through chain entanglement.

The intermediate relaxation time, designated T_{2i} in Figure 6, is due to unentangled polymer chains.[54] The longest relaxation time, T_{2l}, is due to the most mobile sections of chains in the network, particularly dangling chain ends and any free soluble (sol) components that may be present. The NMR T_2 relaxation behavior of PDMS has been extensively studied in the literature for conventional solvents or melts,[53,55,56] and therefore our work has been mainly concerned with the effect of supercritical CO_2 pressure on the transverse relaxation times. Figure 6 shows that all three relaxation times increase with pressure. This is due to the significant swelling of the polymer when exposed to the solvent. The short and intermediate T_2 relaxation times, T_{2s} and T_{2i}, respectively, increase due to the enhanced mobility of the polymer resulting from the increase in free volume within the matrix. For the longest relaxation time, T_{2l}, a significant increase in the value with increasing pressure is observed. This implies that greater mobility is achieved for these chain segments as the CO_2 pressure is increased. T_{2l} is due to protons attached to low-molecular-weight material and chains with high mobility, so it is probable that these chains gain enhanced mobility in supercritical CO_2 with increasing solvent density as the matrix swells.

All of the ^{1}H T_2 relaxation times increased with increasing CO_2 pressure. The proportion of each relaxation time in the decay curve indicates the relative population of chains in each physical environment described above. T_{2l}, which is due to the low-molecular-weight species in the network and chain ends, contributes approximately 25% of the relaxation decay curve at 50 bar. At 300 bar, the contribution to the relaxation decay has risen to about 45% of the total signal. This can be explained by the increase in solubilizing power of the supercritical CO_2 as the density is increased with pressure. As a consequence of this increased density, greater mobility is imparted on all chain segments within the matrix. As the pressure increases, the proportion of chains with high mobility increases at the expense of chains with low mobility. This is due to increasingly larger segments of the polymer chains being able to undergo large-amplitude motions on swelling.

Effect of Exposure of LLDPE to sc-CO_2. To study the effect of supercritical CO_2 pressure on more rigid polymers, high-pressure NMR experiments were performed on a semicrystalline polyolefin, linear low-density poly(ethylene) (LLDPE). It is well-known that supercritical CO_2 does dissolve in LLDPE to a small degree.[2,3] However, no change in polymer dimensions, upon sorption of supercritical CO_2, could be discerned from the NMR imaging experiments. Note that in this experiment the imaging signal arises from the long T_2 component of the transverse magnetization decay, identified below. Supercritical CO_2 does not penetrate the crystalline phase of semicrystalline polyolefins.[2,3] The resolution limit of the NMR experiment is $\approx$20 μm; hence, an increase in dimensions less than this value would be undetectable. Since measurements were performed on films having a thickness of 1 mm, it can be stated that the degree of swelling of LLDPE in supercritical CO_2 must be less than 2%. Despite this lack of observable swelling, the effect of pressure on the polymer chain dynamics could be studied by measuring the ^{1}H transverse relaxation times of the polymer.

The mobility of polymer chains in poly(ethylene) has received considerable attention in the literature due to the economic importance of this family of polymers. Solid-state NMR has provided considerable insight into the molecular motion of polymer chains in the different morphological regions of poly(ethylene). McBrierty[51,52] investigated the nonexponential decay of T_2 relaxation curves for branched and linear poly(ethylene). The study showed that poly(ethylene), whether branched or linear, exhibited numerous relaxation times denoting the different mobility of the polymer chains within the semicrystalline matrix. Kamel and Charlesby[57] have measured the transverse relaxation times for high-density poly(ethylene) at various temperatures and found that the relaxation decays of both the crystalline and amorphous regions of the polymer could be identified. At room temperature, the ^{1}H T_2 relaxation time of protons in the amorphous region is of the order of hundreds of microseconds and from the crystalline region a few tens of microseconds.[57]

^{1}H T_2 relaxation decays for LLDPE were obtained within our high-pressure probe using the CPMG pulse sequence.[33,34] We have been able to measure the proton T_2 relaxation times from the amorphous regions of poly(ethylene); however, the signal from the crystalline protons is obscured by the background signal from the PEEK used in the construction of the high-pressure NMR cell. Consequently, the initial part of the free induction decay from the NMR experiment was discounted. However, the T_2 relaxation times for the amorphous and more mobile protons could be measured with our instrument. For LLDPE at room temperature and pressure, we have been able to resolve three T_2

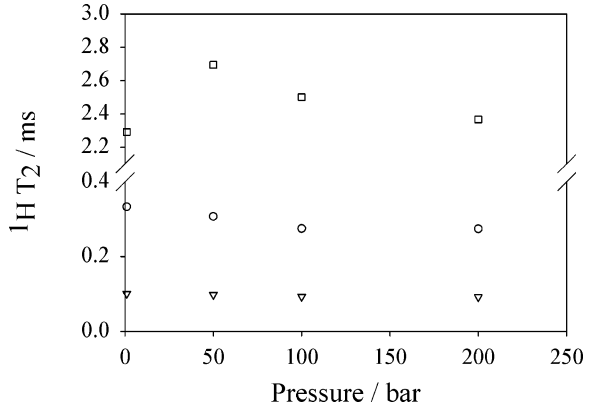

Figure 7. ^{1}H T_2 relaxation times as a function of pressure, for LLDPE swollen in supercritical CO_2 at 45 °C: T_{2s} (triangles), T_{2i} (circles), and T_{2l} (squares).

relaxation times. Two T_2 relaxation times were less than 300 μs and were ascribed to protons in the amorphous region of LLDPE (T_{2s}). The other relaxation time (T_{2l}) was greater than 1 ms (~2% contribution to the signal), which was due either to protons on chains with significantly enhanced mobility or to dangling chain ends.

An investigation into the effect of pressure on the mobility of oligomer chains has been conducted by Prins and co-workers using NMR.[58,59] For amorphous, atactic poly(propylene) pressurized with an inert, nonsolvating gas, it was shown that at a given temperature the rotational correlation time increased as a function of gas density or applied pressure.[59] This indicated a decrease in the mobility of the polymer chains with increasing pressure. Prins and Kulik[60] also investigated the effect of pressure on the mobility of chains in the amorphous region of linear poly(ethylene). Again, an increase in the motional correlation time was observed with increasing pressure, consistent with a decrease in the mobility of chains in the amorphous region under high pressure.

Figure 7 shows the three relaxation times measured for amorphous LLDPE as a function of pressure. The long T_2, corresponding to chain ends, initially increases upon addition of liquid CO_2 at 45 °C. This is due to a slight swelling effect of the liquid. Upon further elevation of the pressure, however, all three relaxation times decrease. Note that the proportion of the three components remains largely unchanged with increasing pressure. Unlike cross-linked PDMS, which gained increasing mobility with pressure due to supercritical CO_2 being a moderately good solvent, the LLDPE chains become more constrained in the amorphous region at higher pressure. This agrees with the observations of Prins and co-workers[58−60] for poly(ethylenes) subjected to pressure by an inert gas. Indeed, the very poor solubility of supercritical CO_2 in LLDPE is shown by the absence of swelling in the NMR images. This low degree of swelling is comparable to that observed in other studies of the behavior of semicrystalline polymers in supercritical CO_2.[45]

Summary

The effect of exposure of cross-linked PDMS and semicrystalline LLDPE to supercritical CO_2 has been examined using high-pressure NMR spectroscopy and imaging. In the case of cross-linked PDMS, a high degree of swelling was observed for all cross-link densities. Equilibrium swelling was found to occur relatively rapidly, within less than 1 h, and the extent of swelling increased with increasing fluid density. The polymer−solvent interaction parameter, χ, was determined, and it was concluded that supercritical CO_2 is a poor solvent for PDMS with a molecular weight of 30 000 Da, when compared to toluene or benzene. The interaction parameter, χ, was found to have a linear dependence on the cross-link density for CO_2 pressures investigated in this work. The polymer chain mobility was enhanced at increasing pressure in all regions of the matrix, as evidenced by increases in the ^{1}H T_2 relaxation times.

In contrast to the rubbery PDMS networks, NMR imaging showed no measurable increase in dimensions of semicrystalline LLDPE upon exposure to supercritical CO_2 at any pressure. This was due to the relatively low sorption of solvent into the polymer compared to PDMS. However, the ^{1}H T_2 relaxation times in the amorphous regions systematically decreased as the pressure was increased. This was related to the strain imposed on the polymer chains by introduction of an external static pressure.

References and Notes

(1) Van der Stegen, G. H. D. D.E.J. International Research Co. B. V.; Neth. Application: DE; 1977; 9 pp.
(2) Thurecht, K. J.; Hill, D. J. T.; Preston, C. M. L.; Rintoul, L.; White, J. L.; Whittaker, A. K. *Macromolecules* **2004**, *37*, 6019−6026.
(3) Watkins, J. J.; McCarthy, T. J. *Macromolecules* **1994**, *27*, 4845−4847.
(4) Walker, T. A.; Raghavan, S. R.; Royer, J. R.; Smith, S. D.; Wignall, G. D.; Melnichenko, Y.; Khan, S. A.; Spontak, J. *J. Phys. Chem. B* **1999**, *103*, 5472−5476.
(5) Kung, E.; Lesser, A. J.; McCarthy, T. J. *Macromolecules* **1998**, *31*, 4160−4169.
(6) Zhang, J.; Busby, A. J.; Roberts, C. J.; Chen, X.; Davies, M. C.; Tendler, S. J. B.; Howdle, S. M. *Macromolecules* **2002**, *35*, 8869−8877.
(7) Watkins, J. J.; McCarthy, T. J. *Chem. Mater.* **1995**, *7*, 1991−1994.
(8) Said-Galiyev, E.; Nikitin, L.; Vinokur, R.; Gallyamov, M.; Kurykin, M.; Petrova, O.; Lokshin, B.; Volkov, I.; Khokhlov, A.; Schaumburg, K. *Ind. Eng. Chem. Res.* **2000**, *39*, 4891−4896.
(9) Zhao, Q.; Samulski, E. T. *Macromolecules* **2003**, *36*, 6967−6969.
(10) Flichy, N. B. M.; Kazarian, S. G.; Lawrence, C. J.; Briscoe, B. J. *J. Phys. Chem. B* **2002**, *106*, 754−759.
(11) Wind, J. D.; Sirard, S. M.; Paul, D. R.; Green, P. F.; Johnston, K. P.; Koros, W. J. *Macromolecules* **2003**, *36*, 6442−6448.
(12) Wynne, K. J.; Shenoy, S.; Fujiwara, T.; Irie, S.; Woerdeman, D.; Sebra, R.; Garach, A.; McHugh, M. *Polym. Prepr.* **2003**, *43*, 888−889.
(13) Thurecht, K. J.; Whittaker, A. K.; Hill, D. J. T. *Macromolecules*, in press.
(14) Liu, Z.; Dong, Z.; Han, B.; Wang, J.; He, J.; Yang, G. *Chem. Mater.* **2002**, *14*, 4619−4623.
(15) Muth, O.; Vogel, H.; Hirth, T. *J. Supercrit. Fluids* **2001**, *19*, 299−306.
(16) DeSimone, J. M.; Gaun, Z.; Elsbernd, C. S. *Science* **1992**, *257*, 945.
(17) Royer, J. R.; DeSimone, J. M.; Khan, S. A. *Macromolecules* **1999**, *32*, 8965−8973.
(18) Shenoy, S. L.; Fujiwara, T.;Wynne, K. J. *Macromolecules* **2003**, *36*, 3380−3385.
(19) Melnichenko, Y. B.; Kiran, E.; Heath, K. D.; Salaniwal, S.; Cochran, H. D.; Stamm, M.; Van Hook, W. A.; Wignall, G. D. *J. Appl. Crystallogr.* **2000**, *33*, 682−685.
(20) Kazarian, S. G.; Chan, K. L. A. *Macromolecules* **2004**, *37*, 579−584.
(21) Ballard, L.; Reiner, C.; Jonas, J. *J. Magn. Reson. A* **1996**, *123*, 81−86.
(22) Bertani, R.; Mali, M.; Roos, J.; Brinkmann, D. *Rev. Sci. Instrum.* **1992**, *63*, 3303−3306.
(23) Dardin, A.; Cain, J. B.; DeSimone, J. M.; Johnson, C. S.; Samulski, E. T. *Macromolecules* **1997**, *30*, 3593−3599.
(24) Niessen, H. G.; Trautner, P.; Wiemman, S.; Bargon, J.; Woelk, K. *Rev. Sci. Instrum.* **2002**, *73*, 1259−1266.

(25) Yamaguchi, T.; Kimura, Y.; Nakahara, M. *J. Phys. Chem. B* **2002**, *106*, 9126−9134.
(26) Demco, D. E.; Blumich, B. *Curr. Opin. Solid State Mater. Sci.* **2001**, *5*, 195−202.
(27) Harding, S. G.; Johns, M. L.; Pugh, S. R.; Fryer, P. J.; Gladden, L. F. *Food Addit. Contam.* **1997**, *14*, 583−589.
(28) Ghi, P. Y.; Hill, D. J. T.; Whittaker, A. K. *Biomacromolecules* **2001**, *2*, 504−510.
(29) Hill, D. J. T.; Preston, C. M. L.; Whittaker, A. K.; Salisbury, D. J. *Radiat. Phys. Chem.* **2001**, *62*, 11−17.
(30) Bremner, T.; Whittaker, A. K. Personal communication, 1995.
(31) Brandrup, J., Immergut, E. H., Eds.; *Polymer Handbook*, 3rd ed.; John Wiley and Sons: New York, 1989.
(32) Wallen, S. L.; Schoenbackler, L. K.; Dawson, E. D.; Blatchford, M. A. *Anal. Chem.* **2000**, *72*, 4230−4234.
(33) Carr, H. Y.; Purcell, E. M. *Phys. Rev.* **1954**, *94*, 630−638.
(34) Meiboom, S.; Gill, D. *Rev. Sci. Instrum.* **1958**, *29*, 688−691.
(35) Charlesby, A. *Proc. R. Soc. London* **1955**, *A230*, 120−135.
(36) Miller, A. A. *J. Am. Chem. Soc.* **1960**, *82*, 3519.
(37) Hill, D. J. T.; Preston, C. M. L.; Whittaker, A. K. *Polymer* **2001**, *43*, 1051−1059.
(38) Hill, D. J. T.; Preston, C. M. L.; Whittaker, A. K.; Hunt, S. M. *Macromol. Symp.* **2000**, *156*, 95−102.
(39) Flory, P. J.; Rehner, J. *J. Chem. Phys.* **1943**, *11*, 521−526.
(40) Malone, S. P.; Vosburgh, C.; Cohen, C. *Polymer* **1993**, *34*, 5149−5153.
(41) Gillmor, J. R.; Colby, R. H.; Patel, S. K.; Malone, S.; Cohen, C. *Macromolecules* **1992**, *25*, 5241−5251.
(42) Fleming, G. K.; Koros, W. J. *Macromolecules* **1986**, *19*, 2285−2291.
(43) Andre, P.; Folk, S. L.; Adam, M.; Rubinstein, M.; DeSimone, J. M. *J. Phys. Chem. A* **2004**, *108*, 9901−9907.
(44) Melnichenko, Y. B.; Kiran, E.; Wignall, G. D.; Heath, K. D.; Salaniwal, S.; Cochran, H. D.; Stamm, M. *Macromolecules* **1999**, *32*, 5344−5347.
(45) Koga, T.; Seo, Y.; Zhang, Y.; Shin, K.; Kusano, K.; Nishikawa, K.; Rafailovich, M. H.; Sokolov, J. C.; Chu, B.; Peiffer, D.; Occhiogrosso, R.; Satija, S. K. *Phys. Rev. Lett.* **2002**, *89*, 1−4.
(46) Tan, Z.; Jaeger, R.; Vancso, G. J. *Polymer* **1994**, *35*, 3230−3236.
(47) Vera-Graziano, R.; Hernandez-Sanchez, F.; Cauich-Rodriguez, J. V. *J. Appl. Polym. Sci.* **1995**, *55*, 1317−1327.
(48) McKenna, G. B.; Flynn, K. M.; Chen, Y. *Polymer* **1990**, *31*, 1937−1945.
(49) Hrnjak-Murgic, Z.; Jelencic, J.; Bravar, M.; Marovic, M. *J. Appl. Polym. Sci.* **1997**, *65*, 991−999.
(50) McKenna, G. B.; Flynn, K. M.; Chen, Y. *Polym. Commun.* **1988**, *29*, 272−275.
(51) McBrierty, V. J. *Polymer* **1974**, *15*, 503−520.
(52) McBrierty, V. J.; McDonald, I. R. *Polymer* **1975**, *16*, 125−133.
(53) Shim, S. E.; Parr, J. C.; von Meerwall, E.; Isayev, A. I. *J. Phys. Chem. B* **2002**, *106*, 12072−12078.
(54) Gussoni, M.; Greco, F.; Mapelli, M.; Vezzoli, A.; Ranucci, E.; Ferruti, P.; Zetta, L. *Macromolecules* **2002**, *35*, 1722−1729.
(55) Folland, R.; Charlesby, A. *Radiat. Phys. Chem.* **1977**, *10*, 61−68.
(56) Menge, H.; Hotopf, S.; Ponitzsch, S.; Richter, S.; Arndt, K.; Schneider, H.; Heuert, U. *Polymer* **1999**, *40*, 5303−5313.
(57) Kamel, I.; Charlesby, A. *J. Polym. Sci., Polym. Phys. Ed.* **1981**, *19*, 803−814.
(58) de Langen, M.; Luigjes, H.; Prins, K. O. *Polymer* **2000**, *41*, 1183−1191.
(59) Hollander, A. G. S.; Prins, K. O. *Int. J. Thermophys.* **2001**, *22*, 357−375.
(60) Kulik, A. S.; Prins, K. O. *Polymer* **1994**, *35*, 2307−2314.

MA0503108